MATHEMATICAL METHODS IN THE APPLIED SCIENCES
Math. Meth. Appl. Sci. 2004; **27**:19–34 (DOI: 10.1002/mma.432)
MOS subject classification: 35 L 05; 65 N 30

A Wiener–Hopf approximation technique for a multiple plate diffraction problem

James R. Brannan[1], Vincent J. Ervin[1,*,†], Jinqiao Duan[2,3] and Leonid Razoumov[4]

[1] *Department of Mathematical Sciences, Clemson University, Clemson, SC 29634-0975, U.S.A.*
[2] *Department of Applied Mathematics, Illinois Institute of Technology, Chicago, IL 60616, U.S.A.*
[3] *Department of Mathematics, The University of Science and Technology of China, Hefei 230026, China*
[4] *Qualcomm Inc., San Diego, CA 92121-2779, U.S.A.*

Communicated by F.-O. Speck

SUMMARY

An approximation method is derived for the computation of the acoustic field between a series of parallel plates, subject to a time periodic incident field. The method is based on the Wiener–Hopf method of factorization, with computations involving orthogonal bases of functions that are analytic in the complex half-plane. Copyright © 2004 John Wiley & Sons, Ltd.

KEY WORDS: Wiener-Hopf; diffraction; orthogonal expansion

1. INTRODUCTION

In this article we combine the classical Wiener–Hopf technique with an orthogonal expansion for holomorphic functions to compute an approximation to the solution of the acoustic field between a series of parallel plates of varying heights and spacings. This problem has received considerable attention throughout the years. An elegant solution for two, semi-infinite plates of equal height, was obtained by Jones in Reference [1], (see also Reference [2]). In Reference [3], Jones presented the solution for three uniformly spaced, semi-infinite soft plates, of equal heights. The solution for two semi-infinite plates with different heights was given by Abrahams and Wickham in Reference [4]. They extended their work in Reference [5] to model scattering of water waves from opposing vertical barriers. In Reference [6] Alkumru considered the case of electromagnetic diffraction from three uniformly spaced, semi-infinite *thick* plates, of equal heights where the plates have non-zero thickness.

The difficulty in extending the Wiener–Hopf technique to the general N-plate setting has been in obtaining a suitable product factorization of the $N \times N$ matrix arising in the method. In Reference [7] Meister *et al.* presented an operator splitting approach to construct a suitable

* Correspondence to: Vincent J. Ervin, Department of Mathematical Sciences, Clemson University, Clemson, South Carolina 29634-0975, U.S.A.
† E-mail: vjervin@clemson.edu

 Received 29 August 2002

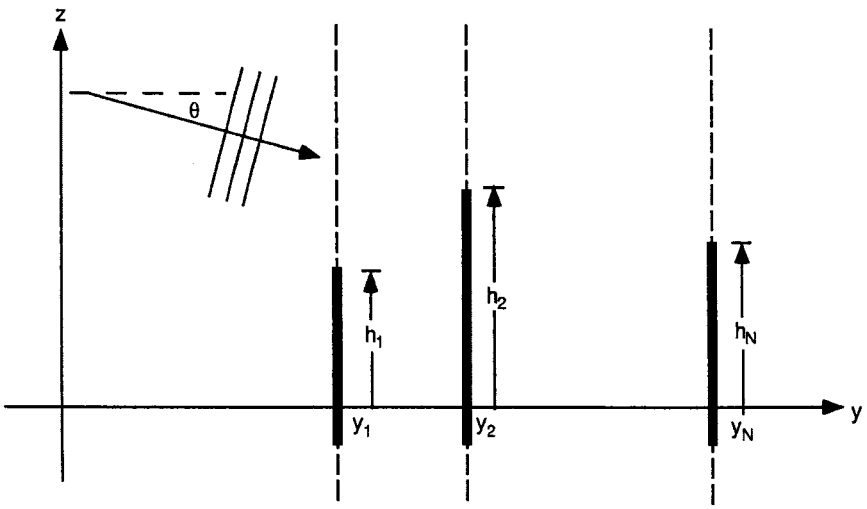

Figure 1. Plane waves incident on a set of parallel plates.

factorization of the associated Fourier symbol, and showed that the Wiener–Hopf system was invertible provided the plates were sufficiently separated.

Our work in this paper extends the approach presented in Reference [1] to the case of N-plates. For our general setting an approximation method is required, as it is still an open research question how to factor the operators associated with the determining equations for the solution into two pieces: one holomorphic in an upper half plane, and the other holomorphic in a lower half plane, with algebraic behaviour at infinity. Using an orthogonal basis for holomorphic functions we present a numerical approximation algorithm for the N-plate problem. Results from the numerical scheme are demonstrated for a 3-plate example.

The multi-plate diffraction problem has recently been considered as a model for predicting radiowave propogation in urban microcell environments [8–12]. (In the case the magnetic (or electric) field of the incoming signal is orientated perpendicular to the direction of propogation of the plane wave, the problem may be recast as the scalar Helmholtz equation.) Several different approaches have been applied to this problem: empirical, semi-empirical, theoretical, ray-tracing and those employing the uniform theory of diffraction [9–11,13].

This paper is organized as follows. In Section 2 we derive the approximating system of equations for the coupled field. The approximation approach to solving these equations is then presented in Section 3. An example demonstrating the technique is given in Section 4.

2. MATHEMATICAL MODEL

The problem investigated in this paper is that of a plane wave field impinging upon a system of N semi-infinite plates, each parallel to the xz-plane and arranged one behind the other along the positive y-axis (Figure 1). The height of the edges of the plates above the xy-plane may vary from plate to plate. We assume that the vector normal to the wavefronts of the incident field is parallel to the yz-plane and makes an angle θ with the positive y-axis.

Assuming an $e^{j\omega t}$ time dependence, the incident field is specified by

$$\phi_{\text{inc}}(y,z) = e^{-jk(y\cos\theta + z\sin\theta)}$$

We partition the yz-plane into $N+1$ subdomains defined by

$$D_0 = \{(y,z) : -\infty < y < y_1, -\infty < z < \infty\}$$
$$D_n = \{(y,z) : y_n < y < y_{n+1}, -\infty < z < \infty\}, \quad n = 1,\ldots,N-1$$

and

$$D_N = \{(y,z) : y_N < y < \infty, -\infty < z < \infty\}$$

If we let $\psi_n(y,z)$ denote the total wave field in domain D_n, then $\psi_n(y,z)$ must satisfy the two-dimensional Helmholtz equation,

$$\frac{\partial^2\psi}{\partial y^2} + \frac{\partial^2\psi}{\partial z^2} + k^2\psi = 0, \quad (y,z) \in D_n \tag{1}$$

for each $n = 0,\ldots,N$. In addition, we impose the following interface conditions:

$$\psi_{n-1}(y_n - 0, z) = \psi_n(y_n + 0, z), \quad h_n < z < \infty, \quad n = 1,\ldots,N \tag{2}$$

$$\frac{\partial\psi_{n-1}(y_n - 0, z)}{\partial y} = \frac{\partial\psi_n(y_n + 0, z)}{\partial y}, \quad h_n < z < \infty, \quad n = 1,\ldots,N \tag{3}$$

$$\frac{\partial\psi_{n-1}(y_n - 0, z)}{\partial y} = 0, \quad -\infty < z < h_n, \quad n = 1,\ldots,N \tag{4}$$

and

$$\frac{\partial\psi_n(y_n + 0, z)}{\partial y} = 0, \quad -\infty < z < h_n, \quad n = 1,\ldots,N \tag{5}$$

Conditions (2) and (3) arise from the requirement that the wavefield and its normal derivative be continuous along the interfaces between regions above the plates. Conditions (4) and (5) constitute a hard boundary condition on both sides of each plate. Note that together conditions (3), (4), and (5) imply that

$$\frac{\partial\psi_{n-1}(y_n - 0, z)}{\partial y} = \frac{\partial\psi_n(y_n + 0, z)}{\partial y}, \quad -\infty < z < \infty, \quad n = 1,\ldots,N \tag{6}$$

In addition to the interface conditions we impose a constraint that disallows waves propagating in from infinity assuming an $e^{j\omega t}$ time dependence, that is, a radiation condition. For the index of refraction we use $k = k_1 - jk_2$ with $0 < k_2 \ll 1$, and requiring solutions to be bounded as y tends to plus infinity. Calculations are simplified if we represent the total wave field in each

domain as a sum of the incident field and a residual field $\phi_n(y,z)$,

$$\psi_n(y,z) = \phi_n(y,z) + \phi_{\text{inc}}(y,z), \quad n = 0,\ldots,N \tag{7}$$

Denote the Fourier transform of $\phi_n(y,z)$ with respect to z by $\Phi_n(y,\lambda)$,

$$\Phi_n(y,\lambda) = \int_{-\infty}^{\infty} \phi_n(y,z)\mathrm{e}^{-\mathrm{j}\lambda z}\,\mathrm{d}z \tag{8}$$

It follows from (1) and the radiation conditions that

$$\Phi_0(y,\lambda) = L_1(\lambda)\mathrm{e}^{\sqrt{\lambda^2-k^2}\,y} \tag{9}$$

$$\Phi_n(y,\lambda) = L_{n+1}(\lambda)\mathrm{e}^{\sqrt{\lambda^2-k^2}\,y} + R_n(\lambda)\mathrm{e}^{-\sqrt{\lambda^2-k^2}\,y}, \quad n = 1,\ldots,N-1 \tag{10}$$

and

$$\Phi_N(y,\lambda) = R_N(\lambda)\mathrm{e}^{-\sqrt{\lambda^2-k^2}\,y} \tag{11}$$

The branch cut for $\sqrt{\lambda-k}$ is taken to be $\{\lambda : \lambda = k - \mathrm{j}\tau,\ 0<\tau<\infty\}$ and the branch cut for $\sqrt{\lambda+k}$ is taken to be $\{\lambda : \lambda = k + \mathrm{j}\tau,\ 0<\tau<\infty\}$. We also specify that $\mathscr{R}e(\sqrt{\lambda^2-k^2})>0$ if $|\mathscr{R}e(\lambda)| > \mathscr{R}e(k)$.

Fourier transforming each of the interface conditions (6) with respect to z and substituting (9)–(11) into the resulting equations yields the following relationships between the left and right propagating mode amplitude functions,

$$L_1(\lambda)\mathrm{e}^{\gamma y_1} = L_2(\lambda)\mathrm{e}^{\gamma y_1} - R_1(\lambda)\mathrm{e}^{-\gamma y_1} \tag{12}$$

$$L_{n+1}(\lambda)\mathrm{e}^{\gamma y_{n+1}} - R_n(\lambda)\mathrm{e}^{-\gamma y_{n+1}} = L_{n+2}(\lambda)\mathrm{e}^{\gamma y_{n+1}} - R_{n+1}(\lambda)\mathrm{e}^{-\gamma y_{n+1}}, \quad n = 1,\ldots,N-2 \tag{13}$$

$$L_N(\lambda)\mathrm{e}^{\gamma y_N} - R_{N-1}(\lambda)\mathrm{e}^{-\gamma y_N} = -R_N(\lambda)\mathrm{e}^{-\gamma y_N} \tag{14}$$

where $\gamma := \sqrt{\lambda^2-k^2}$.

The total wave field in each domain D_n expressed in terms of Fourier integral representations of the $\phi_n(y,z)$ is

$$\psi_0(y,z) = \frac{1}{2\pi}\int_{-\infty}^{\infty} L_1(\lambda)\mathrm{e}^{\gamma y}\mathrm{e}^{\mathrm{j}\lambda z}\,\mathrm{d}\lambda + \phi_{\text{inc}}(y,z) \tag{15}$$

$$\psi_n(y,z) = \frac{1}{2\pi}\int_{-\infty}^{\infty} [L_{n+1}(\lambda)\mathrm{e}^{\gamma y} + R_n(\lambda)\mathrm{e}^{-\gamma y}]\mathrm{e}^{\mathrm{j}\lambda z}\,\mathrm{d}\lambda + \phi_{\text{inc}}(y,z), \quad n = 1,\ldots,N-1 \tag{16}$$

$$\psi_N(y,z) = \frac{1}{2\pi}\int_{-\infty}^{\infty} R_N(\lambda)\mathrm{e}^{-\gamma y}\mathrm{e}^{\mathrm{j}\lambda z}\,\mathrm{d}\lambda + \phi_{\text{inc}}(y,z) \tag{17}$$

If we now apply interface conditions (2) to (15)–(17) and use the relationships (12)–(14) we find that

$$\frac{1}{2\pi}\int_{-\infty}^{\infty} R_1(\lambda)\mathrm{e}^{-\gamma y_1}\mathrm{e}^{\mathrm{j}\lambda h_1}\mathrm{e}^{\mathrm{j}\lambda z}\,\mathrm{d}\lambda = 0, \quad z>0 \tag{18}$$

$$\frac{1}{2\pi}\int_{-\infty}^{\infty} [L_{n+1}(\lambda)-L_n(\lambda)]\mathrm{e}^{\gamma y_n}\mathrm{e}^{\mathrm{j}\lambda h_n}\,\mathrm{e}^{\mathrm{j}\lambda z}\,\mathrm{d}\lambda = 0, \quad z>0, \quad n=1,\ldots,N-1 \tag{19}$$

$$\frac{1}{2\pi}\int_{-\infty}^{\infty} [R_{n+1}(\lambda)-R_n(\lambda)]\mathrm{e}^{-\gamma y_{n+1}}\mathrm{e}^{\mathrm{j}\lambda h_{n+1}}\mathrm{e}^{\mathrm{j}\lambda z}\,\mathrm{d}\lambda = 0, \quad z>0, \quad n=1,\ldots,N-1 \tag{20}$$

and

$$\frac{1}{2\pi}\int_{-\infty}^{\infty} L_N(\lambda)\mathrm{e}^{\gamma y_N}\mathrm{e}^{\mathrm{j}\lambda h_N}\mathrm{e}^{\mathrm{j}\lambda z}\,\mathrm{d}\lambda = 0, \quad z>0 \tag{21}$$

Any argument similar to that of Reference [2, p. 101], see Appendix B, shows that

$$R_1(\lambda)\mathrm{e}^{-\gamma y_1}\mathrm{e}^{\mathrm{j}\lambda h_1}$$

$$[L_{n+1}(\lambda)-L_n(\lambda)]\mathrm{e}^{\gamma y_n}\mathrm{e}^{\mathrm{j}\lambda h_n}, \quad n=1,\ldots,N-1$$

$$[R_{n+1}(\lambda)-R_n(\lambda)]\mathrm{e}^{-\gamma y_{n+1}}\mathrm{e}^{\mathrm{j}\lambda h_{n+1}}, \quad n=1,\ldots,N-1$$

and

$$L_N(\lambda)\mathrm{e}^{\gamma y_N}\mathrm{e}^{\mathrm{j}\lambda h_N}$$

are analytic functions of λ for $\mathscr{I}m(\lambda) > k_2\sin\theta$ and are $O(|\lambda|^{-1})$ as $|\lambda|\to\infty$. We therefore set

$$E_1^{(+)}(\lambda) := R_1(\lambda)\mathrm{e}^{-\gamma y_1}\mathrm{e}^{\mathrm{j}\lambda h_1} = (L_2(\lambda)-L_1(\lambda))\mathrm{e}^{\gamma y_1}\mathrm{e}^{\mathrm{j}\lambda h_1}, \quad \text{(using 12)} \tag{22}$$

$$\begin{aligned} E_{n+1}^{(+)}(\lambda) &:= [R_{n+1}(\lambda)-R_n(\lambda)]\mathrm{e}^{-\gamma y_{n+1}}\mathrm{e}^{\mathrm{j}\lambda h_{n+1}} \\ &= [L_{n+2}(\lambda)-L_{n+1}(\lambda)]\mathrm{e}^{\gamma y_{n+1}}\mathrm{e}^{\mathrm{j}\lambda h_{n+1}}, \quad n=1,\ldots,N-2 \end{aligned} \tag{23}$$

$$\begin{aligned} E_N^{(+)}(\lambda) &:= [R_{n+1}(\lambda)-R_n(\lambda)]\mathrm{e}^{-\gamma y_N}\mathrm{e}^{\mathrm{j}\lambda h_N} \\ &= L_N(\lambda)\mathrm{e}^{\gamma y_N}\mathrm{e}^{\mathrm{j}\lambda h_N} \end{aligned} \tag{24}$$

where the superscript plus signs indicate that the functions are analytic in the upper half space and tend to zero as $|\lambda|\to\infty$.

The interface conditions (4)–(5) applied to (15)–(17) yield the coupled system of $2N$ integral equations

$$\frac{1}{2\pi}\int_{-\infty}^{\infty}\sqrt{\lambda^2-k^2}L_1(\lambda)\mathrm{e}^{\gamma y_1}\mathrm{e}^{\mathrm{j}\lambda h_1}\mathrm{e}^{\mathrm{j}\lambda z}\,\mathrm{d}\lambda = \mathrm{j}k\cos\theta\mathrm{e}^{-\mathrm{j}k(y_1\cos\theta+(z+h_1)\sin\theta)},\quad z<0 \tag{25}$$

$$\frac{1}{2\pi}\int_{-\infty}^{\infty}\sqrt{\lambda^2-k^2}[L_{n+1}(\lambda)\mathrm{e}^{\gamma y_n}-R_n(\lambda)\mathrm{e}^{-\gamma y_n}]\mathrm{e}^{\mathrm{j}\lambda h_n}\mathrm{e}^{\mathrm{j}\lambda z}\,\mathrm{d}\lambda$$
$$= \mathrm{j}k\cos\theta\mathrm{e}^{-\mathrm{j}k(y_n\cos\theta+(z+h_n)\sin\theta)},\quad z<0,\quad n=1,\ldots,N-1 \tag{26}$$

$$\frac{1}{2\pi}\int_{-\infty}^{\infty}\sqrt{\lambda^2-k^2}[L_{n+1}(\lambda)\mathrm{e}^{\gamma y_{n+1}}-R_n(\lambda)\mathrm{e}^{-\gamma y_{n+1}}]\mathrm{e}^{\mathrm{j}\lambda h_{n+1}}\mathrm{e}^{\mathrm{j}\lambda z}\,\mathrm{d}\lambda$$
$$= \mathrm{j}k\cos\theta\mathrm{e}^{-\mathrm{j}k(y_{n+1}\cos\theta+(z+h_{n+1})\sin\theta)},\quad z<0,\quad n=1,\ldots,N-1 \tag{27}$$

and

$$-\frac{1}{2\pi}\int_{-\infty}^{\infty}\sqrt{\lambda^2-k^2}R_N(\lambda)\mathrm{e}^{-\gamma y_N}\mathrm{e}^{\mathrm{j}\lambda h_N}\mathrm{e}^{\mathrm{j}\lambda z}\,\mathrm{d}\lambda$$
$$= \mathrm{j}k\cos\theta\mathrm{e}^{-\mathrm{j}k(y_N\cos\theta+(z+h_N)\sin\theta)},\quad z<0 \tag{28}$$

Note, in view of (12)–(14), Equations (26), (28), are equivalent to (25), (27).

Define

$$g_1(z)=\begin{cases}\dfrac{1}{2\pi}\displaystyle\int_{-\infty}^{\infty}\sqrt{\lambda^2-k^2}L_1(\lambda)\mathrm{e}^{\gamma y_1}\mathrm{e}^{\mathrm{j}\lambda h_1}\,\mathrm{e}^{\mathrm{j}\lambda z}\,\mathrm{d}\lambda & z>0\\ 0 & z<0\end{cases} \tag{29}$$

$$g_{n+1}(z)=\begin{cases}\dfrac{1}{2\pi}\displaystyle\int_{-\infty}^{\infty}\sqrt{\lambda^2-k^2}[L_{n+1}(\lambda)\mathrm{e}^{\gamma y_{n+1}}-R_n(\lambda)\mathrm{e}^{-\gamma y_{n+1}}]\mathrm{e}^{\mathrm{j}\lambda h_{n+1}}\mathrm{e}^{\mathrm{j}\lambda z}\,\mathrm{d}\lambda & z>0\\ 0 & z<0\end{cases} \tag{30}$$

for $n=1,\ldots,N-1$. We now Fourier transform (25), (27) to obtain the system of equations

$$\sqrt{\lambda^2-k^2}L_1(\lambda)\mathrm{e}^{\gamma y_1}\mathrm{e}^{\mathrm{j}\lambda h_1} = -\frac{k\cos\theta}{\lambda+k\sin\theta}\,\mathrm{e}^{-\mathrm{j}k(y_1\cos\theta+h_1\sin\theta)}+G_1^{(-)}(\lambda) \tag{31}$$

$$\sqrt{\lambda^2-k^2}[L_{n+1}(\lambda)\mathrm{e}^{\gamma y_{n+1}}-R_n(\lambda)\mathrm{e}^{-\gamma y_{n+1}}]\mathrm{e}^{\mathrm{j}\lambda h_{n+1}}$$
$$= -\frac{k\cos\theta}{\lambda+k\sin\theta}\,\mathrm{e}^{-\mathrm{j}k(y_{n+1}\cos\theta+h_{n+1}\sin\theta)}+G_{n+1}^{(-)}(\lambda),\quad n=1,\ldots,N-1 \tag{32}$$

where the functions $G_n^{(-)}(\lambda)$, the Fourier transforms of $g_n(z)$, for $n=1,\ldots,N$, are holomorphic in the lower half plane $\mathscr{I}m(\lambda)<k_2$, see Appendix C, and are $O(|\lambda|^{-1/2})$ as $|\lambda|\to-\infty$.

In order for the transforms (31)–(32) to exist it is necessary that $\mathscr{I}m(\lambda)>k_2\sin\theta$. Consequently, inversion contours for (31)–(32) must pass below the branch point at $\lambda=-k$ and above the branch point at $\lambda=k$ and the pole at $\lambda=-k\sin\theta$.

Introduce the matrix notation $\mathbf{R}(\lambda)=[R_1(\lambda),\ldots,R_N(\lambda)]^{\mathrm{T}}, \mathbf{L}(\lambda)=[L_1(\lambda),\ldots,L_N(\lambda)]^{\mathrm{T}}$, $a_n(\lambda)=\mathrm{e}^{\gamma y_n}$,

$$\mathbf{A}(\lambda)=\begin{bmatrix} a_1(\lambda) & 0 & \cdots & 0 \\ a_1(\lambda) & a_2(\lambda) & \cdots & 0 \\ \vdots & \vdots & \ddots & \vdots \\ a_1(\lambda) & a_2(\lambda) & \cdots & a_N(\lambda) \end{bmatrix} \tag{33}$$

$$\mathbf{B}(\lambda)=\begin{bmatrix} a_1^{-1}(\lambda) & a_2^{-1}(\lambda) & \cdots & a_N^{-1}(\lambda) \\ 0 & a_2^{-1}(\lambda) & \cdots & a_N^{-1}(\lambda) \\ \vdots & \vdots & \ddots & \vdots \\ 0 & 0 & \cdots & a_N^{-1}(\lambda) \end{bmatrix} \tag{34}$$

and

$$\mathbf{P}(\lambda)=\begin{bmatrix} \mathrm{e}^{\mathrm{j}\lambda h_1} & 0 & \cdots & 0 \\ 0 & \mathrm{e}^{\mathrm{j}\lambda h_2} & \cdots & 0 \\ \vdots & \vdots & \ddots & \vdots \\ 0 & 0 & \cdots & \mathrm{e}^{\mathrm{j}\lambda h_N} \end{bmatrix} \tag{35}$$

Note that (12)–(14) may be expressed in matrix form as

$$\begin{aligned} \mathbf{B}^{-1}(\lambda)\mathbf{L}(\lambda)&=-\mathbf{A}^{-1}(\lambda)\mathbf{R}(\lambda) \\ \Rightarrow \mathbf{L}(\lambda)&=-\mathbf{B}(\lambda)\mathbf{A}^{-1}(\lambda)\mathbf{R}(\lambda) \end{aligned} \tag{36}$$

and from (22)–(24)

$$\mathbf{E}^{(+)}(\lambda)=\mathbf{P}(\lambda)\mathbf{A}^{-1}(\lambda)\mathbf{R}(\lambda) \tag{37}$$

Equations (31)–(32) can be rewritten as

$$-\sqrt{\lambda^2-k^2}[\mathbf{I}+\mathbf{P}(\lambda)(\mathbf{C}(\lambda)+\mathbf{C}^{\mathrm{T}}(\lambda))\mathbf{P}^{-1}(\lambda)]\mathbf{E}^{(+)}(\lambda)=-\frac{k\cos\theta}{\lambda+k\sin\theta}\,\mathbf{b}+\mathbf{G}^{(-)}(\lambda) \tag{38}$$

where

$$\mathbf{E}^{(+)}(\lambda)=\begin{bmatrix}E_1^{(+)}\\ \vdots\\ E_N^{(+)}\end{bmatrix},\quad \mathbf{G}^{(-)}(\lambda)=\begin{bmatrix}G_1^{(-)}\\ \vdots\\ G_N^{(-)}\end{bmatrix},\quad \mathbf{b}=\begin{bmatrix}\mathrm{e}^{-\mathrm{j}k(y_1\cos\theta+h_1\sin\theta)}\\ \vdots\\ \mathrm{e}^{-\mathrm{j}k(y_N\cos\theta+h_N\sin\theta)}\end{bmatrix} \tag{39}$$

and

$$\mathbf{C}(\lambda)=\begin{bmatrix}0 & a_1(\lambda)a_2^{-1}(\lambda) & a_1(\lambda)a_3^{-1}(\lambda) & \dots & a_1(\lambda)a_N^{-1}(\lambda)\\ 0 & 0 & a_2(\lambda)a_3^{-1}(\lambda) & \dots & a_2(\lambda)a_N^{-1}(\lambda)\\ \vdots & \vdots & \vdots & \ddots & \vdots\\ 0 & 0 & 0 & \dots & a_{N-1}(\lambda)a_N^{-1}(\lambda)\\ 0 & 0 & 0 & \dots & 0\end{bmatrix} \tag{40}$$

If we now define

$$\hat{\mathbf{G}}^{(-)}(\lambda)=\frac{1}{\sqrt{\lambda+k}}\,\mathbf{G}^{(-)}(\lambda) \tag{41}$$

then Equation (38) may be written as

$$\sqrt{\lambda-k}[\mathbf{I}+\mathbf{P}(\lambda)(\mathbf{C}(\lambda)+\mathbf{C}^{\mathrm{T}}(\lambda))\mathbf{P}^{-1}(\lambda)]\mathbf{E}^{(+)}(\lambda)=\frac{k\cos\theta}{(\lambda+k\sin\theta)\sqrt{\lambda+k}}\,\mathbf{b}-\hat{\mathbf{G}}^{(-)}(\lambda) \tag{42}$$

Splitting the first term on the right hand side of (42) into a sum of two functions, one holomorphic in the upper half plane and the other holomorphic in the lower half plane, we rewrite (42) as

$$\begin{aligned}&\sqrt{\lambda-k}[\mathbf{I}+\mathbf{P}(\lambda)(\mathbf{C}(\lambda)+\mathbf{C}^{\mathrm{T}}(\lambda))\mathbf{P}^{-1}(\lambda)]\mathbf{E}^{(+)}(\lambda)\\ &\quad=\frac{\cos\theta}{\lambda+k\sin\theta}\,\frac{\sqrt{k}}{\sqrt{1-\sin\theta}}\,\mathbf{b}+\mathbf{H}^{(-)}(\lambda)\end{aligned} \tag{43}$$

where

$$\mathbf{H}^{(-)}(\lambda)=\frac{k\cos\theta}{\lambda+k\sin\theta}\left[\frac{1}{\sqrt{\lambda+k}}-\frac{1}{\sqrt{k(1-\sin\theta)}}\right]\mathbf{b}-\hat{\mathbf{G}}^{(-)}(\lambda) \tag{44}$$

In the classical Wiener–Hopf approach one would now factor the term in front of $\mathbf{E}^{(+)}$ into a product of two functions, one holomorphic in the upper half plane and the other holomorphic in the lower half plane, with algebraic behaviour at infinity. However, for the general setting considered in this paper such a decomposition is not known. We therefore proceed by computing a numerical approximation to the solution of (43).

3. NUMERICAL APPROXIMATION

3.1. Functions holomorphic in a half-plane

Let $\alpha > 0$ and consider the system of functions

$$\omega_m(\eta) = \sqrt{\frac{\alpha}{\pi}} \frac{(\eta - j\alpha)^{m-1}}{(\eta + j\alpha)^m}, \quad \omega_{-m}(\eta) = \sqrt{\frac{\alpha}{\pi}} \frac{(\eta + j\alpha)^{m-1}}{(\eta - j\alpha)^m}, \quad m = 1, 2, 3, \ldots \tag{45}$$

Restricting the domain of the functions to the real axis, the system (45) is a complete orthonormal system for $\mathscr{L}_p(-\infty, \infty)$, $1 < p < \infty$ [14], equipped with the inner product

$$\langle f, g \rangle = \int_{-\infty}^{\infty} f(\eta) \bar{g}(\eta) \, \mathrm{d}\eta$$

Furthermore, functions $E(\eta)$ which are holomorphic in the upper half plane with boundary values in $\mathscr{L}_p(-\infty, \infty)$ have a unique representation

$$E(\eta) = \sum_{m=1}^{\infty} e_m \omega_m(\eta)$$

where the Fourier coefficients e_n are obtained from the boundary values of E on the real axis,

$$e_m = \int_{-\infty}^{\infty} E(\eta) \bar{\omega}_m(\eta) \, \mathrm{d}\eta, \quad m = 1, 2, 3, \ldots$$

Similarly, functions $F(\eta)$ holomorphic in the lower half plane with boundary values in $\mathscr{L}_p(-\infty, \infty)$ have a unique representation

$$F(\eta) = \sum_{m=1}^{\infty} f_{-m} \omega_{-m}(\eta)$$

Note that from (22)–(24), and (B7)–(B9), along the real axes $\sqrt{\lambda - k} E_n^+(\lambda) \in \mathscr{L}_p(-\infty, \infty)$, for $p > 2$. Illustrated in Figures 2 and 3, are the real and imaginary parts of $\omega_2(\eta)$ and $\omega_7(\eta)$, respectively.

3.2. Projection onto functions analytic in a half-plane

With k expressed in complex polar coordinates as $k = \rho_k \omega_k$ where $\rho_k = |k|$ and $\omega_k = \mathrm{e}^{\mathrm{j}\arg(k)}$, and using the scalings $\lambda = \rho_k \eta$, $\tilde{\mathbf{E}}^{(+)}(\eta) = \rho_k \mathbf{E}^{(+)}(\rho_k \eta)$, $\tilde{\mathbf{P}}(\eta) = \mathbf{P}(\rho_k \eta)$, $\tilde{\mathbf{C}}(\eta) = \mathbf{C}(\rho_k \eta)$, and $\tilde{\mathbf{H}}^{(-)}(\eta) = \sqrt{\rho_k} \mathbf{H}^{(-)}(\rho_k \eta)$, then (43) may be rewritten as

$$\sqrt{\eta - w_k} [\mathbf{I} + \tilde{\mathbf{P}}(\eta)(\tilde{\mathbf{C}}(\eta) + \tilde{\mathbf{C}}^{\mathrm{T}}(\eta)) \tilde{\mathbf{P}}^{-1}(\eta)] \tilde{\mathbf{E}}^{(+)}(\eta)$$

$$= \frac{\sqrt{w_k} \cos\theta}{(\eta + w_k \sin\theta) \sqrt{1 - \sin\theta}} \mathbf{b} + \tilde{\mathbf{H}}^{(-)}(\eta) \tag{46}$$

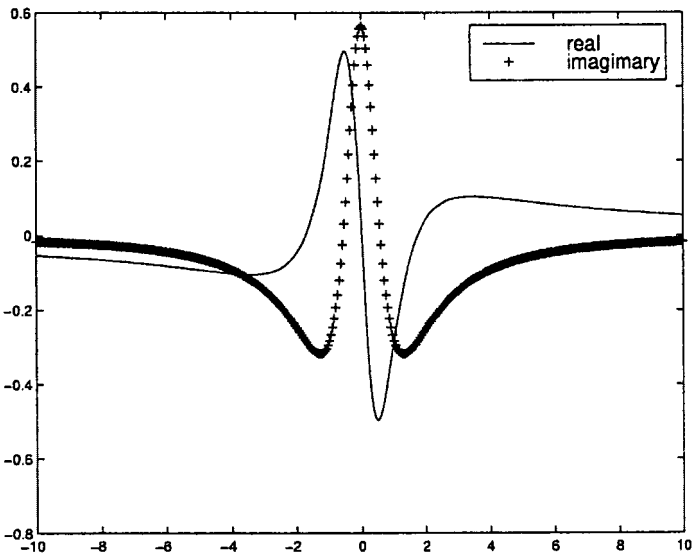

Figure 2. Real and imaginary parts of $\omega_2(\eta)$.

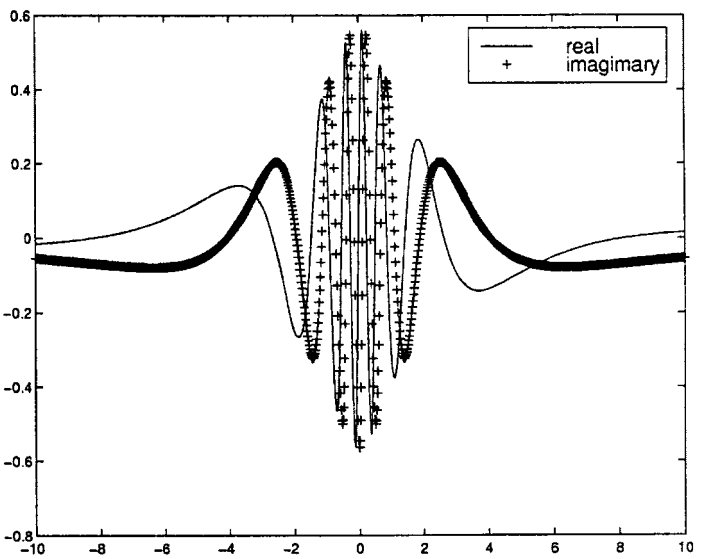

Figure 3. Real and imaginary parts of $\omega_7(\eta)$.

We seek to solve for the approximation

$$\sqrt{\eta - w_k}\tilde{\mathbf{E}}^{(+)}(\eta) = \sum_{m=1}^{M} \mathbf{e}_m \omega_m(\eta) \tag{47}$$

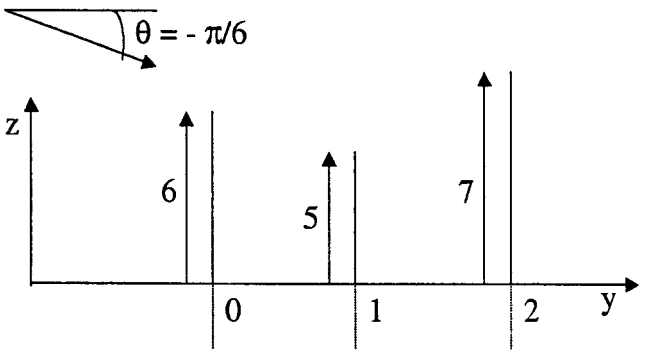

Figure 4. Configuration of plates and incoming wave.

Substituting (47) into (46), followed by taking inner products on both sides with $\tilde{\omega}_v(\eta)$, $v = 1, 2, 3, \ldots, M$, yields the finite-dimensional system

$$\mathbf{e}_v + \sum_{m=1}^{M} S_{vm}\mathbf{e}_m = \frac{\sqrt{w_k}\cos\theta}{\sqrt{1-\sin\theta}}\, s_v \mathbf{b}, \quad v = 1, \ldots, M \tag{48}$$

where

$$S_{vm} = Q_{vm} + R_{vm} = \int_{-\infty}^{\infty} \tilde{\mathbf{P}}(\eta)[\tilde{\mathbf{C}}(\eta) + \tilde{\mathbf{C}}^{\mathrm{T}}(\eta)]\tilde{\mathbf{P}}^{-1}(\eta)\omega_m(\eta)\bar{\omega}_v(\eta)\,\mathrm{d}\eta \tag{49}$$

and

$$s_v = \int_{-\infty}^{\infty} \frac{\bar{\omega}_v(\eta)}{(\eta + w_k \sin\theta)}\,\mathrm{d}\eta$$

Solving (48) for $\mathbf{e}_v$, $v = 1, \ldots, M$, we then use (47), (37), (36), (9)–(11), (7), to approximate the total acoustic field.

4. NUMERICAL ILLUSTRATION OF THE METHOD

In this section we present an example illustrating the method presented above. We consider the case of three parallel plates located at $y_1 = 0$, $y_2 = 1$, and $y_3 = 2$, with heights $h_1 = 6$, $h_2 = 5$, and $h_3 = 7$, respectively (see Figure 4). The values for k and θ used were $k = 20 - \mathrm{j}0.05$ and $\theta = -\pi/6$. Presented in Figures 5–9 is $|\psi_n(y,z)|/|\phi_{\mathrm{inc}}(y,z)|$, plotted over a region containing the three plates, and also for each of the regions between and outside the plates.

Note that the plot in Figure 6 is consistent with the sum of the incoming wave plus the reflected wave with the maximum and minimum values occurring where expected. The plot in Figure 9 is also consistent with what is expected for a signal in a 'shadow' region.

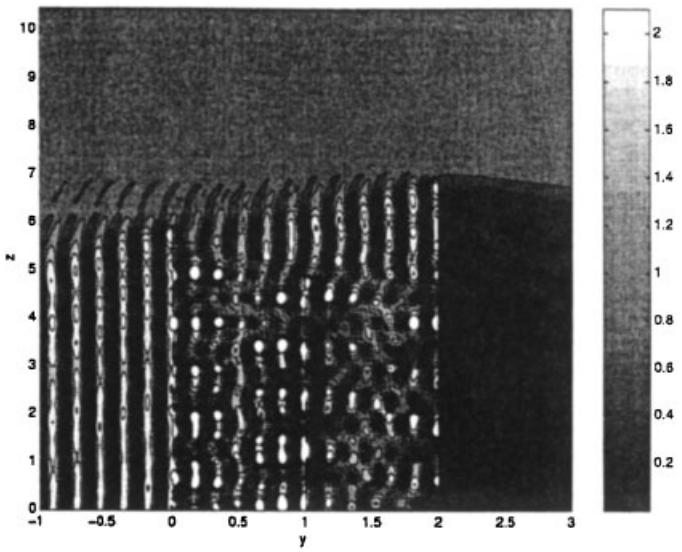

Figure 5. $|\psi_n(y,z)|/|\phi_{\text{inc}}(y,z)|$ over the entire region.

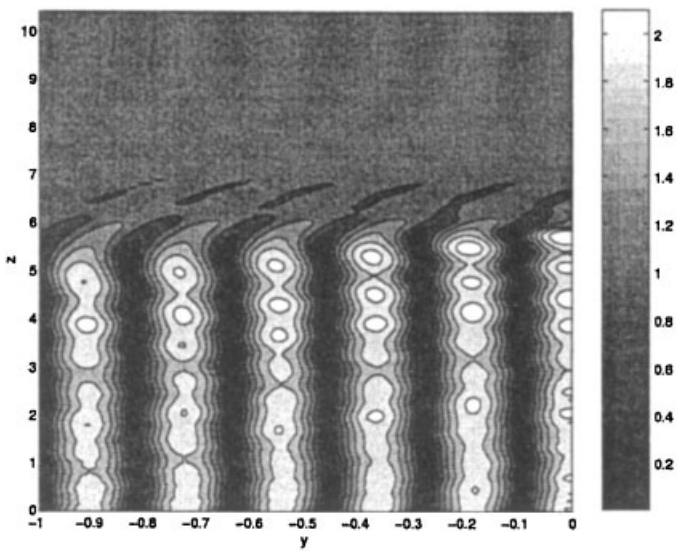

Figure 6. $|\psi_n(y,z)|/|\phi_{\text{inc}}(y,z)|$ in front of plate 1.

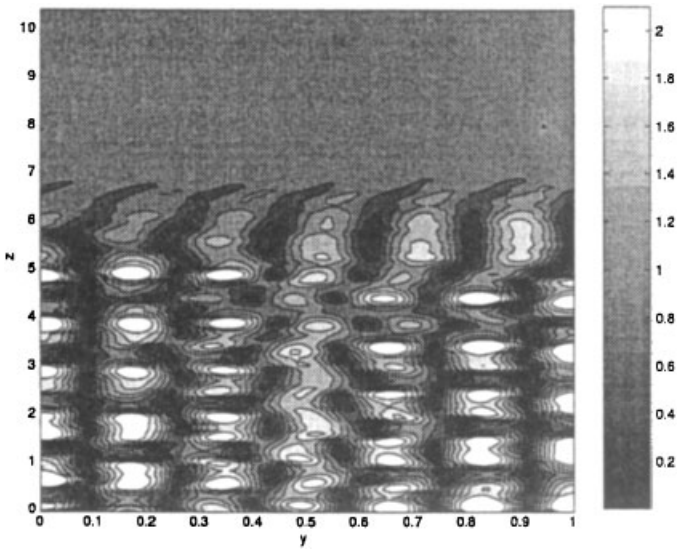

Figure 7. $|\psi_n(y,z)|/|\phi_{\text{inc}}(y,z)|$ between plates 1 and 2.

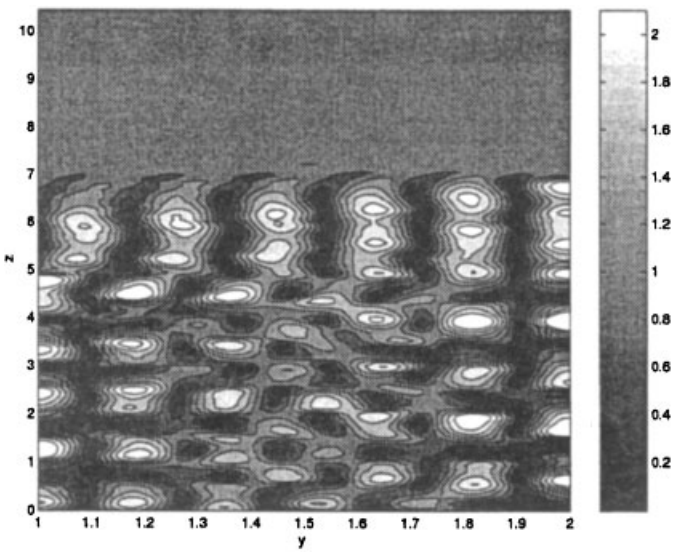

Figure 8. $|\psi_n(y,z)|/|\phi_{\text{inc}}(y,z)|$ between plates 2 and 3.

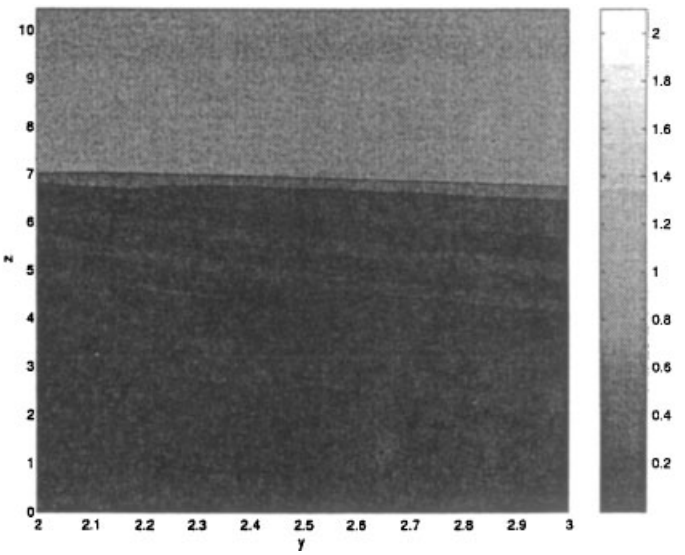

Figure 9. $|\psi_n(y,z)|/|\phi_{\text{inc}}(y,z)|$ behind plate 3.

APPENDIX A: BEHAVIOUR OF $\phi_n(y,z)$

Following the discussion of Noble [2, p. 100], we have the following behaviour for $\phi_n(y,z)$:

$$\lim_{r\to 0^+} \phi_n(y_i, h_i + r) = O(1), \quad \lim_{r\to 0^+} \frac{\partial \phi_n}{\partial y}(y_i, h_i + r) = O(r^{-1/2}),$$
$$\text{for } n = 0,\ldots,N, \text{ and } i = n, n+1 \tag{A1}$$

For any fixed $y, -\infty < y < \infty$,

$$|\phi| < C_1 \mathrm{e}^{-k_2 z} \text{ as } z \to \infty, \quad \text{and} \quad |\phi| < C_2 \mathrm{e}^{-k_2 \sin\theta z} \text{ as } z \to -\infty \tag{A2}$$

APPENDIX B: BEHAVIOUR OF $(L_{n+1} - L_n)\mathrm{e}^{\sqrt{\lambda^2-k^2}\,y_n}\mathrm{e}^{\mathrm{j}\lambda h_n}$ AND $(R_n - R_{n-1})\mathrm{e}^{-\sqrt{\lambda^2-k^2}\,y_n}\mathrm{e}^{\mathrm{j}\lambda h_n}$

In view of $\Phi_n(y,\lambda)$ defined by (8), we introduce the following notation:

$$\Phi_n^+(y_i) := \Phi_n^+(y_i,\lambda) = \int_{h_i}^{\infty} \phi_n(y_n, z)\mathrm{e}^{-\mathrm{j}\lambda z}\,\mathrm{d}z$$
$$= \mathrm{e}^{-\mathrm{j}\lambda h_i}\int_0^{\infty} \phi_n(y_n, z + h_i)\mathrm{e}^{-\mathrm{j}\lambda z}\,\mathrm{d}z, \quad i = n, n+1 \tag{B1}$$

$$\Phi_n^-(y_i) := \Phi_n^-(y_i,\lambda) = \int_{-\infty}^{h_i} \phi_n(y_n,z)\mathrm{e}^{-\mathrm{j}\lambda z}\,\mathrm{d}z$$
$$= \mathrm{e}^{-\mathrm{j}\lambda h_i}\int_{\infty}^{0} \phi_n(y_n,z+h_i)\mathrm{e}^{-\mathrm{j}\lambda z}\,\mathrm{d}z, \quad i=n,n+1 \tag{B2}$$

From (A2) it follows that $\Phi_n^+(y_i)$ is analytic for $Re(\lambda)<k_2$, and $\Phi_n^-(y_i)$ is analytic for $Re(\lambda)>k_2\sin\theta$.

In addition, from the Abelian theorems, [2, p. 36], we have that

$$\Phi_n^+(y_i)=O(|\lambda|^{-1}), \quad \Phi_n^-(y_i)=O(|\lambda|^{-1}) \quad \text{as } |\lambda|\to\infty \tag{B3}$$

Comparing (8)–(11) with (B1), (B2) we have:

$$\begin{aligned}\Phi_0^+(y_1)+\Phi_0^-(y_1) &= L_1(\lambda)\mathrm{e}^{\sqrt{\lambda^2-k^2}y_1}\\ \Phi_1^+(y_1)+\Phi_1^-(y_1) &= L_2(\lambda)\mathrm{e}^{\sqrt{\lambda^2-k^2}y_1}+R_1(\lambda)\mathrm{e}^{-\sqrt{\lambda^2-k^2}y_1}\end{aligned} \tag{B4}$$

$$\left.\begin{aligned}\Phi_{n-1}^+(y_n)+\Phi_{n-1}^-(y_n) &= L_n(\lambda)\mathrm{e}^{\sqrt{\lambda^2-k^2}y_n}+R_{n-1}(\lambda)\mathrm{e}^{-\sqrt{\lambda^2-k^2}y_n}\\ \Phi_n^+(y_n)+\Phi_n^-(y_n) &= L_{n+1}(\lambda)\mathrm{e}^{\sqrt{\lambda^2-k^2}y_n}+R_n(\lambda)\mathrm{e}^{-\sqrt{\lambda^2-k^2}y_n}\end{aligned}\right\} \quad n=2,\ldots,N-1 \tag{B5}$$

$$\begin{aligned}\Phi_{N-1}^+(y_N)+\Phi_{N-1}^-(y_N) &= L_N(\lambda)\mathrm{e}^{\sqrt{\lambda^2-k^2}y_N}+R_{N-1}(\lambda)\mathrm{e}^{-\sqrt{\lambda^2-k^2}y_N}\\ \Phi_N^+(y_N)+\Phi_N^-(y_N) &= R_N(\lambda)\mathrm{e}^{-\sqrt{\lambda^2-k^2}y_N}\end{aligned} \tag{B6}$$

Using the fact that $\phi_{n-1}(y_n,z)=\phi_n(y_n,z)$ for $z>h_n$, $n=1,\ldots,N$, we have $\Phi_{n-1}^+(y_n)=\Phi_n^+(y_n)$. Hence, subtracting the equations in (B4), (B5), and (B6) yields

$$\Phi_1^-(y_1)-\Phi_0^-(y_1)=(L_2(\lambda)-L_1(\lambda))\mathrm{e}^{\sqrt{\lambda^2-k^2}y_1}+R_1(\lambda)\mathrm{e}^{-\sqrt{\lambda^2-k^2}y_1}$$
$$\Phi_n^-(y_n)-\Phi_{n-1}^-(y_n)=(L_{n+1}(\lambda)-L_n(\lambda))\mathrm{e}^{\sqrt{\lambda^2-k^2}y_n}+(R_n(\lambda)-R_{n-1}(\lambda))\mathrm{e}^{-\sqrt{\lambda^2-k^2}y_n}$$
$$\Phi_N^-(y_N)-\Phi_{N-1}^-(y_N)=-L_N(\lambda)\mathrm{e}^{\sqrt{\lambda^2-k^2}y_N}+(R_N(\lambda)-R_{N-1}(\lambda))\mathrm{e}^{-\sqrt{\lambda^2-k^2}y_N}$$

Next, using (12)–(14), implies

$$\begin{aligned}\Phi_1^-(y_1)-\Phi_0^-(y_1) &= 2(L_2(\lambda)-L_1(\lambda))\mathrm{e}^{\sqrt{\lambda^2-k^2}y_1}\\ &= 2R_1(\lambda)\mathrm{e}^{-\sqrt{\lambda^2-k^2}y_1}\end{aligned} \tag{B7}$$

$$\begin{aligned}\Phi_n^-(y_n)-\Phi_{n-1}^-(y_n) &= 2(L_{n+1}(\lambda)-L_n(\lambda))\mathrm{e}^{\sqrt{\lambda^2-k^2}y_n}\\ &= 2(R_n(\lambda)-R_{n-1}(\lambda))\mathrm{e}^{-\sqrt{\lambda^2-k^2}y_n}\end{aligned} \tag{B8}$$

$$\Phi_N^-(y_N) - \Phi_{N-1}^-(y_N) = -2L_N(\lambda)\mathrm{e}^{\sqrt{\lambda^2-k^2}\,y_N}$$
$$= 2(R_N(\lambda) - R_{N-1}(\lambda))\mathrm{e}^{-\sqrt{\lambda^2-k^2}\,y_N} \tag{B9}$$

Thus, in view of the behaviour of $\Phi_n^-(y_i)$ described above, we have that the function on the RHS of (B7)–(B9), are all analytic for $Re(\lambda) > k_2 \sin\theta$, and are $O(|\lambda|^{-1})$ as $|\lambda| \to \infty$.

APPENDIX C: BEHAVIOUR OF $G_n^-(\lambda)$

We discuss the case of $G_n^-(\lambda)$. Below $\mathscr{F}^{-1}$ denotes the inverse Fourier transform, and $'$ differentiation with respect to y.

From (29), (30) observe that

$$g_n(z) = \mathscr{F}^{-1}(\Phi_n^{+\prime}(y_n)) = \begin{cases} \frac{\partial\phi_n(y_n,z)}{\partial y}, & z > h_n \\ 0, & z < h_n \end{cases} \tag{C1}$$

In view of the behaviour of $\partial\phi_n(y_n,z)/\partial y$, (A1), and the Abelian theorems, [2, p. 36], we have that $G_n^-(\lambda)$ is analytic for $Re(\lambda) < k_2$ and has $O(|\lambda|^{-1/2})$ behaviour as $|\lambda| \to \infty$.

REFERENCES

1. Jones DS. A simplifying technique in the solution of a class of diffraction problems. *Quarterly Journal of Mathematics* 1952; **3**(2):189–196.
2. Noble B. *Methods Based on the Wiener–Hopf Technique*. Pergamon Press: New York, 1958.
3. Jones DS. Diffraction by three semi-infinite planes. *Proceedings of the Royal Society of London*, *Series A* 1986; **404**:299–321.
4. Abrahams ID, Wickham GR. On the scattering of sound by two semi-infinite parallel staggered plates. I Explicit matrix Wiener–Hopf factorization. *Proceedings of the Royal Society of London*, *Series A* 1988; **420**:131–156.
5. Abrahams ID, Wickham GR. The scattering of water waves by two semi-infinite opposed vertical walls. *Wave Motion* 1991; **14**:145–168.
6. Alkumru A. Plane wave diffraction by three parallel thick impedance half-planes. *Journal of Electromagnetic Waves and Applications* 1998; **12**:801–819.
7. Meister E, Rottbrand K, Speck F-O. Wiener–Hopf equations for waves scattered by a series of parallel Sommerfeld half-planes. *Mathematical Methods in the Applied Sciences* 1991; **14**:525–552.
8. Bertoni HL, Walfisch J. A theoretical model of UHF propagation in urban environments. *IEEE Transactions on Antennas and Propagations* 1988; **AP-88**:1788–1796.
9. Brown PG, Constantinou CC. Investigations on the prediction of radiowave propagation in urban microcell environments using ray-tracing methods. *IEE Proceedings—Microwaves*, *Antennas and Propagations* 1996; **143**:36–42.
10. Grosskopf R. Prediction of urban propagation loss. *IEEE Transactions on Antennas and Propagation* 1994; **42**:658–665.
11. Ikegami F, Takeuchi T, Yoshida S. Theoretical prediction of mean field strength for urban mobile radio. *IEEE Transactions on Antennas and Propagation* 1991; **39**:299–302.
12. Saunders SR, Bonar FR. Explicit multiple building diffraction attenuation function for mobile radio wave propagation. *Electronics Letters* 1991; **27**:1276–1277.
13. Anderson JB. Transition zone diffraction by multiple edges. *IEE Proceedings—Microwaves*, *Antennas and Propagations* 1994; **141**:382–384.
14. Hille E. *Analytic Function Theory*, vol. II, Ginn and Company: Boston, 1962.

